S21A-0131 An energy-duration procedure for rapid and accurate determination of earthquake magnitude and tsunamigenic potential

Anthony Lomax

A Lomax Scientific, Mouans-Sartoux, France; anthony@alomax.net, www.alomax.net

Alberto Michelini and Alessio Piatanesi

Istituto Nazionale di Geofisica e Vulcanologia (INGV), Roma, Italy; www.ingv.it

1. Introduction

The 26 December 2004, M9 Sumatra-Andaman earthquake caused a tsunami that devastated Indian Ocean coasts within 3 hours; the 17 July 2006, M_w=7.7 Java earthquake caused an unexpectedly large and destructive tsunami. For both events the magnitude and other information available within the first hour after the origin time (OT) severely underestimated the event size and tsunamigenic potential. Improved tsunami warning and emergency response for future large earthquakes requires that accurate knowledge of the earthquake size and tsunamigenic potential is available rapidly, within 30 minutes or less after OT. There are a number of procedures for rapid analysis of large earthquakes in use at earthquake and tsunami monitoring centers. For example, the Pacific Tsunami Warning Center (PTWC) uses the M_{wp} moment magnitude and the M_m mantle magnitude. Currently, however, the earliest accurate estimates of the size of large earthquakes are moment tensor determinations, including the Harvard Centroid-Moment Tensor (CMT) (*e.g.*, Dziewonski et al., 1981), based on long-period, *S* and surface-wave recordings, typically not available until and hour or more after OT.

Seismic *P* waves are the earliest signal to arrive at seismic recording stations. At teleseismic distances the arrival times of the initial *P*-wave are used routinely to locate the earthquake hypocentre within about 15 minutes after OT. The *P*-waves also contains comprehensive information about the event size and source character. **Here we introduce a rapid and robust, energy-duration procedure to obtain an earthquake moment and a moment magnitude, M_{ED}, from *P*-wave recordings from global seismic stations at 30° to 90° distance from an event. At many earthquake and tsunami monitoring centers, these recordings are available within 20 to 30 minutes after OT. The energy-duration procedure combines a radiated seismic energy measured within the *P* to *S* interval on broadband records, and a source duration measured on high-frequency, *P*-wave records. The measured values also provide the energy-to-moment ratio Θ (*e.g.*, Newman, and Okal, 1998) for identification of tsunami earthquakes.**

2. Theory

Haskell (1964) proposed a kinematic, double-couple, extended-fault model with scalar moment M_0 and a trapezoidal, far-field, source-time function of duration T_0 and rise / fall time xT_0. With this model, Vassiliou and Kanamori (1982) show that the radiated seismic energy, *E*, can be expressed as,

$$E=\left[\frac{1}{15\pi\rho\alpha^5}+\frac{1}{10\pi\rho\beta^5}\right]\frac{2}{x(1-x)^2}\frac{M_0^2}{T_0^3}\ , \tag{1}$$

where *ρ*, *α* and *β* are the density, and *P* and *S* wave speeds, respectively, at the source. **Solving Eq. (1) for M_0 we find, for a given rise-time factor, *x*, a moment estimate,**

$$M_0=K\,x^{1/2}(1-x)E^{1/2}T_0^{3/2}\ , \tag{2}$$

where *K* depends on *ρ*, *α* and *β* at the source. This compact expression (Eq. 2) shows that the scalar moment, M_0, for an earthquake can be obtained from estimates of the radiated energy, *E*, and the source duration, T_0.

3. Methodology

For each earthquake we require a hypocentre location and *P* and *S* travel times from the hypocentre to each station; currently, monitoring agencies have this information within about 10 minutes of OT for teleseismic events (great-circle distance (GCD) to recording stations > ~30°). We use vertical-component, broadband, digital seismograms for about 10 or more stations at 30° to 90° GCD from the source, moderately well distributed in distance and azimuth.

Estimating the radiated seismic energy

An estimate of the radiated seismic energy, *E*, for a point, double-couple source using a *P*-wave seismogram is given by (*e.g.*, Boatwright and Choy, 1986),

$$E=53\pi r^2\rho\alpha\int v^2(t)\,dt\ , \tag{3}$$

where *v*(*t*) is a ground-velocity seismogram, *r* is the source-station distance, and *ρ* and *α* are the density and *P* wave speed, respectively, at the station; the constant terms include corrections for the *P* wave radiation pattern, free-surface amplification and attenuation. **We estimate *E* for each event using the following procedure (Fig. 1):** 1) Convert each seismogram to ground-velocity in m/sec. 2) Cut the seismogram from 10 seconds before the P arrival to 10 seconds before the S arrival to obtain *P*-wave seismograms. 3) Apply (Eq. 3) to each *P* wave seismograms to obtain station energy values. 4) Multiply the station energy value by a factor T_0 / $t_{S\text{-}P}$ if $T_0 > t_{S\text{-}P}$. 5) Calculate an average *E* and associated standard deviation for each event from the station energy values.

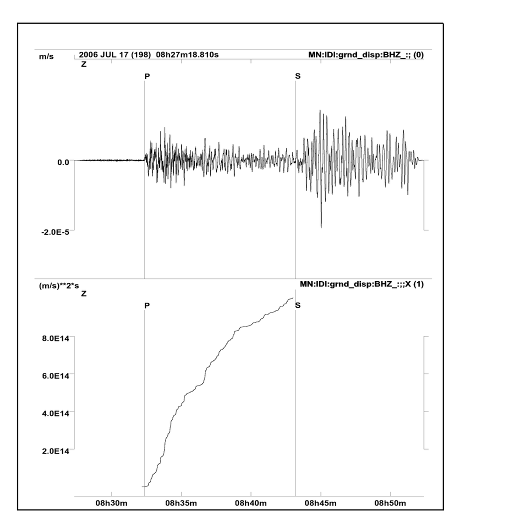

Figure 1. Estimating the radiated seismic energy *E*. Upper trace: ground velocity; Lower: seismogram integrated fro *P* to *S* using (Eq. 5).

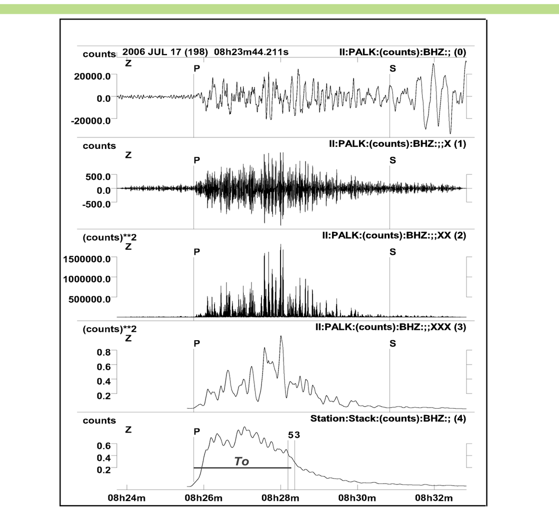

Figure 2. Estimating the the source duration T_0. Trace (0): velocity seismogram; Trace (1): 1 Hz seismogram; Trace (2): velocity-squared; Trace (3): smoothed velocity-squared; Trace (4): stacked, smoothed velocity-squared time-series from all stations; *5* and *3* mark P_{end} times at 50% and 33% of the peak value.

Estimating the source duration T_0

To estimate the source duration, T_0 we make three assumptions: 1) the radiated *P*-waves contain higher frequencies than other wave types; 2) this signal can be isolated on the seismograms; 3) a meaningful time for the end of this signal can be determined. **We estimate T_0 for each event using the following procedure (Fig. 2), based on that of Lomax (2005) and Lomax and Michelini (2005):** 1) Convert the seismograms from each station to high-frequency records using a narrow-band, Gaussian filter of the form $e^{-\alpha\left[(f-f_{cent})/f\right]^2}$, where *f* is frequency, f_{cent} the filter center frequency, and *α* sets the filter width (here we use f_{cent}=1.0 Hz and *α*=10.0). 2) Convert each high-frequency record to kinetic-energy density by squaring the velocity values. 3) Smooth each velocity-squared time-series with a 10 sec wide, triangle function and normalize to form an envelope function. 4) Stack the station envelope functions aligned on their *P* arrival times to form a summary, event envelope function . 5) Measure a source end time, T_{end}, defined as the mean of the times where the event envelope function last drops below 50% and below 33% of its peak value. 6) Calculate the source duration T_0 from the difference between T_{end} and the stack alignment *P* time.

Energy-duration moment and magnitude calculation

From the obtained values of the radiated seismic energy, *E*, and the source duration, T_0, we calculate an energy-duration estimate of the seismic moment, M_0^{ED}, using Eq. (2). We evaluate the unknown rise-time, *x*, through regression of our M_0^{ED} values for each event against the corresponding CMT moment values, M_0^{CMT}, so that the mean of $\log_{10}(M_0^{ED}/M_0^{CMT}) \rightarrow 0$. **Finally we calculate an energy-duration magnitude, M_{ED}, through application of the standard moment to moment magnitude relation,**

$$M_{ED}=(\log_{10}M_0^{ED}-9.1)/1.5\ , \tag{4}$$

where M_0^{ED} has units of N-m.

Energy-to-moment ratio

From the obtained values of the radiated seismic energy, *E*, and our calculated seismic moment estimate, M_0^{ED}, we can determine the energy-to-moment ratio parameter, Θ, (*e.g.*, Newman, and Okal, 1998) for identification of tsunami earthquakes,

$$\Theta=\log_{10}\frac{E}{M_0^{ED}}\ . \tag{5}$$

4. Application to recent large earthquakes

We apply our energy-duration methodology to 35 recent earthquakes with M_w^{CMT}=6.6-9.0 (Table 1). For each event, we obtain from the IRIS Data Center broadband vertical (BHZ) recordings at stations from 30º to 90º GCD. Equivalent data sets would be available within 30 minutes after a large earthquake. Applying the methodology outlined above, excluding poor quality data, we determine *E*, T_0, M_0^{ED}, M_{ED} and Θ for each event (Table 1).

			NEIC				CMT				this study, energy-duration results						
Origin time	Event	Type*	latitude (°)	longitude (°)	depth (km)	Es (N-m)	depth (km)	M_0^{CMT} (N-m)	M_w^{CMT}	T_0† (sec)	T_0 (sec)	E (N-m)	E corrected (N-m)	M_0^{ED} (N-m)	M_{ED}	Θ	M_{wp}
1992.09.02 00:15	**Nicaragua**	**T**	**11.74**	**-87.34**	**44**	**2.6E+14**	**15**	**3.4E+20**	**7.6**	**37**	**175**	**1.9E+14**	**1.9E+14**	**4.4E+20**	**7.7**	**-6.4**	**7.3**
1992.12.12 05:29	Flores Indonesia	I	-8.48	121.9	49	6.6E+15	20	5.1E+20	7.8	36	91	7.8E+15	7.8E+15	1.1E+21	8.0	-5.1	7.7
1993.07.12 13:17	Hokkaido	I	42.85	139.2	18	8.7E+15	17	4.7E+20	7.7	33	78	1.0E+16	1.0E+16	9.8E+20	7.9	-5.0	7.6
1994.01.17 12:30	S California	R	34.21	-118.54	21	1.1E+14	17	1.2E+19	6.7	11	17	1.2E+14	1.2E+14	8.9E+18	6.6	-4.9	6.9
1994.06.02 18:17	**Java**	**T**	**-10.48**	**112.84**	**6**	**1.2E+14**	**15**	**5.3E+20**	**7.7**	**23**	**97**	**3.8E+14**	**3.8E+14**	**2.6E+20**	**7.5**	**-5.8**	**7.5**
1994.06.09 00:33	Bolivia	D	-13.84	-67.55	631	3.2E+16	647	2.6E+21	8.2	40	42	4.8E+16	4.8E+16	3.0E+21	8.2	-4.8	7.8
1994.10.04 13:23	Kuril	P	43.77	147.32	61	1.1E+17	68	3.0E+21	8.3	50	67	6.4E+16	6.4E+16	3.3E+21	8.3	-4.7	7.8
1995.12.03 18:01	Kuril	I	44.66	149.3	23	2.4E+15	26	8.2E+20	7.9	28	71	2.9E+15	2.9E+15	7.5E+20	7.9	-5.4	7.6
1996.02.17 05:59	Irian Jaya	I	-0.89	136.95	11	8.5E+15	15	2.4E+21	8.2	59	114	8.9E+15	8.9E+15	1.6E+21	8.1	-5.3	-
1996.02.21 12:51	**Peru**	**T**	**-9.59**	**-79.59**	**4**	**-**	**15**	**2.2E+20**	**7.5**	**21**	**75**	**2.2E+14**	**2.2E+14**	**1.4E+20**	**7.4**	**-5.8**	**7.3**
1998.07.17 08:49	Papua New Guinea	I	-2.96	141.93	7	2.4E+14	15	3.7E+19	7.1	15	49	1.2E+14	1.2E+14	5.2E+19	7.1	-5.6	6.9
1999.04.08 13:10	Russia-China	D	43.61	130.35	576	9.0E+14	575	5.1E+19	7.1	17	11	7.3E+14	7.3E+14	4.4E+19	7.0	-4.8	7.0
1999.08.17 00:01	Turkey	S	40.75	29.86	13	8.1E+15	17	2.9E+20	7.6	41	51	1.2E+15	1.2E+16	4.6E+20	7.7	-4.6	7.6
1999.09.20 17:47	Taiwan	R	23.77	120.98	8	1.5E+15	21	3.4E+20	7.6	40	58	2.7E+15	2.7E+15	2.6E+20	7.5	-5.0	7.6
1999.10.16 09:46	S California	S	34.59	-116.27	20	1.9E+15	15	6.0E+19	7.1	20	42	1.5E+14	1.5E+15	1.2E+20	7.3	-4.9	7.4
2000.10.06 04:30	W Honshu	S	35.46	133.13	10	2.9E+15	15	1.2E+19	6.7	12	54	4.8E+13	4.8E+14	9.9E+19	7.3	-5.3	6.8
2001.01.26 03:16	S India	R	23.42	70.23	10	6.4E+15	20	3.4E+20	7.6	48	33	7.6E+15	7.6E+15	1.9E+20	7.5	-4.4	7.8
2001.02.28 18:54	Washington	P	47.15	-122.73	-	1.1E+14	51	1.9E+19	6.8	12	15	1.1E+14	1.1E+14	1.4E+19	6.7	-5.1	6.6
2001.03.24 06:27	W Honshu	P	34.08	132.53	-	5.5E+13	47	1.9E+19	6.8	12	34	7.4E+13	7.4E+13	4.1E+19	7.0	-5.7	7.0
2001.06.23 20:33	Peru	I	-16.27	-73.64	8	2.9E+16	30	4.7E+21	8.4	86	135	1.5E+16	1.5E+16	4.5E+21	8.4	-5.5	7.5
2002.11.03 22:12	Alaska	RS	63.52	-147.44	4	3.3E+16	15	7.5E+20	7.9	47	39	2.8E+15	2.8E+16	4.6E+20	7.7	-4.2	7.4
2003.05.21 18:44	N Algeria	R	36.96	3.63	9	3.4E+14	15	2.0E+19	6.8	12	28	2.2E+14	2.2E+14	2.5E+19	6.9	-5.1	7.0
2003.09.25 19:50	Hokkaido	I	41.82	143.91	13	2.2E+16	28	3.1E+21	8.3	67	74	1.4E+16	1.4E+16	1.8E+21	8.1	-5.1	7.9
2003.09.27 11:33	Siberia	S	50.04	87.81	1	5.1E+15	15	9.4E+19	7.2	12	68	5.7E+14	5.7E+15	4.8E+20	7.7	-4.9	7.4
2003.12.26 01:56	S Iran	S	29	58.31	10	6.1E+14	15	9.3E+18	6.6	10	31	3.2E+13	3.2E+14	3.5E+19	7.0	-5.0	6.7
2004.12.23 14:59	Macquarie	S	-50.15	160.37	-	5.2E+16	28	1.6E+21	8.1	53	59	8.3E+15	8.3E+16	3.1E+21	8.3	-4.6	7.8
2004.12.26 00:58	**Sumatra-Andaman**	**IT?**	**3.3**	**95.98**	**39**	**1.4E+17**	**29**	**4.0E+22**	**9.0**	**190**	**420**	**1.4E+17**	**1.4E+17**	**7.7E+22**	**9.2**	**-5.7**	**8.1**
2005.03.28 16:09	N Sumatra	I	2.09	97.11	-	6.7E+16	30	1.1E+22	8.6	99	94	5.0E+16	5.0E+16	4.8E+21	8.4	-5.0	8.2
2005.06.13 22:44	Chile	W	-19.99	-69.2	115	5.4E+15	95	5.1E+20	7.7	36	53	1.6E+16	1.6E+16	1.1E+21	8.0	-4.8	7.6
2005.07.24 15:42	Nicobar	S	7.92	92.19	16	1.2E+16	12	8.8E+19	7.2	25	39	8.4E+14	8.4E+15	2.5E+20	7.5	-4.5	7.2
2005.08.16 02:46	Honshu	I	38.28	142.04	36	3.8E+14	37	7.4E+19	7.2	20	53	3.2E+14	3.2E+14	1.6E+20	7.4	-5.7	7.4
2005.10.08 03:50	Pakistan	R	34.54	73.59	26	3.1E+15	12	2.9E+20	7.6	18	54	2.8E+15	2.8E+15	2.4E+20	7.5	-4.9	7.6
2006.02.22 22:19	Mozambique	N	-21.32	33.58	11	4.4E+14	12	4.5E+19	7.0	16	26	6.4E+14	6.4E+14	3.7E+19	7.0	-4.8	7.3
2006.05.16 10:39	Kermadec	D	31.78	179.31	151	-	155	1.7E+20	7.4	25	25	5.6E+15	5.6E+15	2.2E+20	7.5	-4.6	7.5
2006.07.17 08:19	**Java**	**T**	**-9.25**	**107.41**	**34**	**3.2E+14**	**20**	**4.0E+20**	**7.7**	**100**	**157**	**6.6E+14**	**6.6E+14**	**7.1E+20**	**7.8**	**-6.0**	**7.2**

* **Earthquake type:** I - interplate thrust; **T - tsunami earthquake**; W - downdip; P - intraplate; D - deep; S - strike-slip crustal; R - reverse-faulting crustal; N - normal-faulting crustal.
† 2 x CMT half-duration

Table 1. Events used in this study.

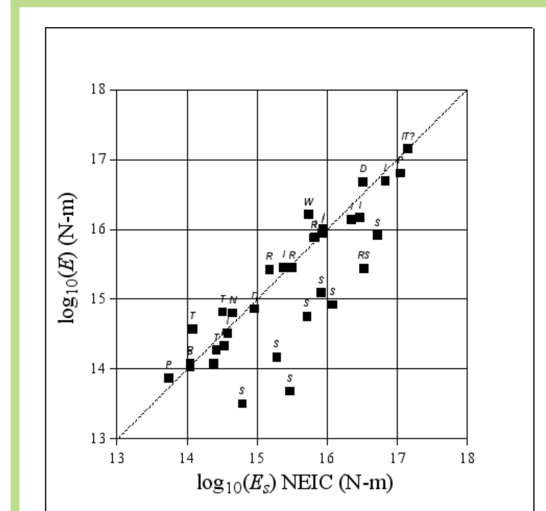

Figure 3. Estimated radiated energy, *E*, from this study compared to E_S determined by the NEIC (Table 1). Events labeled by source type (see Table 1).

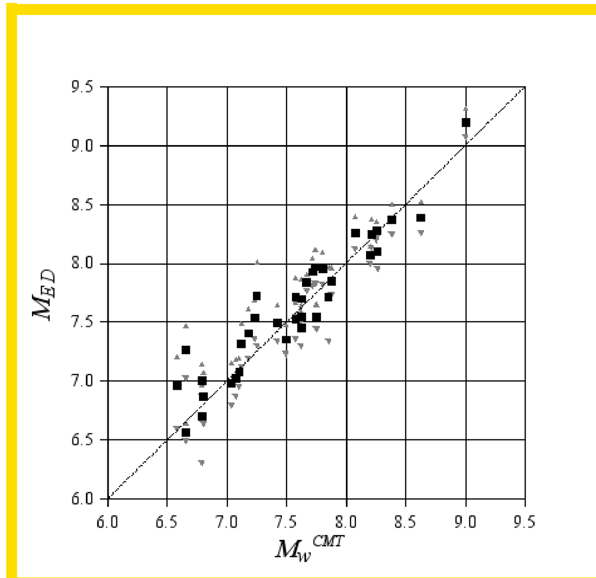

Figure 4. Energy-duration magnitude M_{ED} from this study compared to CMT magnitude M_w^{CMT}. Bounds on M_{ED} are indicated by grey triangles.

Energy estimations

Table 1 and Fig. 3 show that our values, *E*, for radiated energy, excluding strike-slip events, agree well with the radiated energy values, E_S, determined by the NEIC using the procedure of Boatwright and Choy (1986). For all the studied strike-slip earthquakes, however, we obtain *E* values that are less than those of NEIC by a factor of about 10, on average (Table 1, Fig. 5). All of these events have steeply dipping nodal axes close to which teleseismic *P* rays depart from the source; to allow meaningful comparison of our results with CMT values, we increase our radiated seismic energy values, *E*, by a factor of 10 for strike slip events to approximately account for this energy underestimate (Table 1, *E* corrected).

Duration estimations

A comparison between our estimates of source duration T_0 and the CMT duration (*i.e.*, 2 x the CMT half-duration; Table 1) shows that our T_0 values are on average about twice the CMT duration. **Our mean value of T_0=420s and 33% envelope peak value of T_0=473s for 2004.12.26 Sumatra-Andaman are closer than the CMT duration of 190s to the inferred value for the full, co-seismic rupture of about 450-600s for this event (*e.g.* Lomax, 2005; Ammon, *et al.*, 2005). Thus for the larger events, at least, our T_0 values may be good estimates of the duration of co-seismic faulting.** For the smaller events (M_w < ~7) the T_0 values are subject to relatively large uncertainty, since the duration of faulting can be less than the *P* coda length on the high-frequency seismograms (e.g., Fig. 1, lower trace) and of the same order as the width of the smoothing function used to generate the envelope functions.

Moment and energy-duration magnitude calculation

To evaluate the seismic moment, M_0^{ED}, using Eq. 2, we use for each event the *ρ*, *α* and *β* values for the PREM model (Dziewonski and Anderson, 1981) at the CMT centroid depth for the event. Using these values we can compare directly our results to the corresponding M_0^{CMT} and M_w^{CMT} estimates. We calibrate the unknown rise-time factor, *x*, in Eq. 2. through regression of M_0^{ED} against M_0^{CMT}, excluding all strike-slip events.

Our seismic moment estimates, M_0^{ED}, and energy-duration magnitudes, M_{ED}, necessarily correspond to the M_0^{CMT} and M_w^{CMT} values (Table 1, Fig. 4) since we calibrate M_0^{ED} against M_0^{CMT}. More important is the small scatter and low standard-deviation (σ=0.16 magnitude units) of M_{ED} relative to M_w^{CMT}, and the very good match between M_{ED} and M_w^{CMT} for individual events at all magnitudes (Table 1, Fig. 4), including great earthquakes and the 2004, M9 Sumatra-Andaman earthquake (2004.12.26 Sumatra-Andaman; M_w^{CMT}=9.0, M_{ED}=9.2). These results indicate that a rapidly determined, M_{ED} value can provide a robust and accurate estimate of the moment magnitude of future, large earthquakes, including the largest, great events.

Fig. 4 shows increased uncertainty in M_{ED} and increased differences between M_{ED} and M_w^{CMT} for the smallest events (M_w < ~7). These increases are to be expected since there is a relatively large uncertainty in our T_0 estimates for smaller events (recall that M_{ED} a is a function of $T_0^{3/2}$, *c.f.* Eq. 2) and because these events have a wide variety of source types, including strike-slip events, for which our radiated energy estimates can be unstable.

Energy-to-moment ratio Θ

Our energy-to-moment ratio values, Θ, (Table 1) are close to the values of Newman and Okal (1998; their Θ^T values) for the corresponding events. Fig. 5 shows $\log_{10}E$ vs. $\log_{10}M_0^{ED}$ and two important lines of constant Θ.

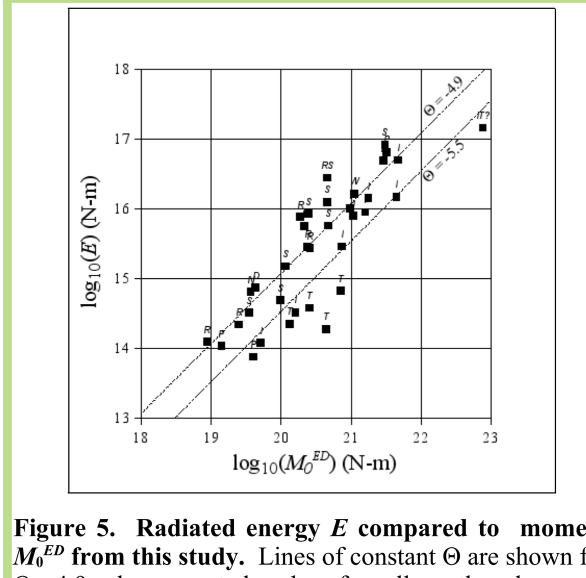

Figure 5. Radiated energy *E* compared to moment M_0^{ED} from this study. Lines of constant Θ are shown for Θ=-4.9, the expected value for all earthquakes, and Θ=-5.5, below which indicates a possible tsunami earthquake. Events labeled by source type (see Table 1).

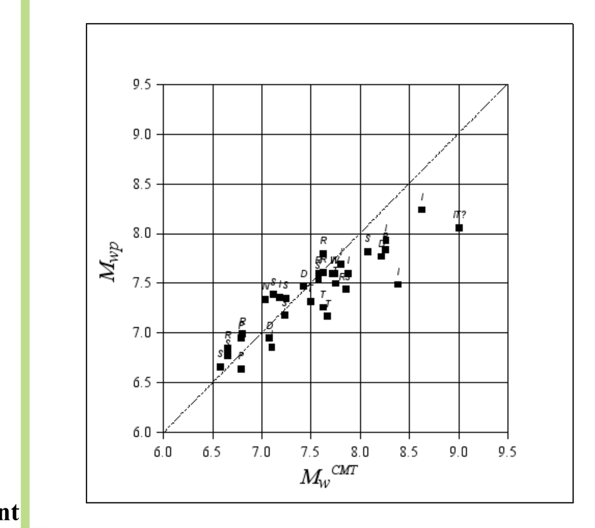

Figure 6. Broadband, moment magnitude M_{wp} from this study compared to CMT magnitude M_w^{CMT}. Events labeled by source type (see Table 1).

5. Discussion

Comparison of M_{ED} and M_w^{CMT}

The energy-duration analysis introduced in this paper, when applied to a set of recent, large earthquakes (M_w^{CMT}=6.6-9.0), produces an energy-duration magnitude, M_{ED} which differ from M_w^{CMT} by less than 0.25 magnitude units for most events at all magnitudes, including the largest great earthquakes (Table 1, Fig. 4). Thus the M_{ED} magnitude is accurate and apparently does not saturate for large events, as does, for example, the M_s surface wave magnitude at about M_s=7.5. These results indicate that the robust, energy-duration procedure and magnitude, M_{ED}, can give rapid, accurate and useful quantification of size for future large and great earthquakes.

The robustness and accuracy of our energy-duration procedure can be attributed to the combined use of two quasi-independent measures, of energy and duration, which quantify different physical characteristics of an earthquake. In addition, the energy-duration procedure uses broadband and high-frequency signals, which typically have higher signal-to-noise levels and little instability relative to the long-period, narrow-band or integrated signals required by most other non-saturating methods for magnitude determination of major and great earthquakes.

Comparison with M_{wp}

The M_{wp} moment magnitude (Tsuboi *et al.*, 1995; Tsuboi *et al.*,1999; Tsuboi, 2000) is calculated from integrated, vertical-component, displacement seismograms containing the *P* and *pP* waves. Because M_{wp} is currently in use for rapid earthquake size assessment (*e.g.* at the PTWC) and can be determined as fast or faster than M_{ED}, we examine here recalculated M_{wp} magnitudes for the studied events (Table 1, Fig. 6). These results, and those of Tsuboi *et al.* (1999) and Hirshorn (2006), show that M_{wp} matches closely M_w^{CMT} up to M_w^{CMT}≈7.5, while above this magnitude M_{wp} tends to underestimate M_w^{CMT}. This M_{wp} underestimate occurs for 2004.12.26 Sumatra-Andaman (M_w^{CMT}=9.0, M_{ED}=9.2, M_{wp}=8.1), and the 2006.07.17 Java, tsunami earthquake (M_w^{CMT}=7.7, M_{ED}=7.8, M_{wp}=7.2), but less for 2005.03.28 Sumatra (M_w^{CMT}=8.6, M_{ED}=8.4, M_{wp}=8.2). These M_{wp} values are consistent with the rapid, M_{wp} estimates of the PTWC (8.0, 7.2 and 8.5, respectively). These results indicate that M_{wp} can saturate above M_w^{CMT}≈7.5, and suggest that some of the largest, M_{wp} underestimates of M_w^{CMT} occur for tsunami earthquakes and tsunamigenic events (*e.g.* 1992.09.02 Nicaragua, 2001.06.23 Peru, 2004.12.26 Sumatra-Andaman, and 2006.07.17 Java). In contrast, we find a good match between M_{ED} and M_w^{CMT} for all events above M_w^{CMT}≈7.0, including great and tsunami earthquakes (Table 1, Fig. 6). **Thus M_{wp} can provide rapid and accurate magnitude estimates for events smaller than M_w^{CMT}≈7.5, while M_{ED}, at teleseismic distances, may be an optimal method to provide rapid and accurate magnitude estimates for events larger than M_w^{CMT}≈7.0.**

Energy-to-moment ratio Θ and tsunami earthquakes

The energy-to-moment ratio, Θ, is an important discriminant for potential tsunami earthquakes (*e.g.*, Newman, and Okal, 1998). The energy-to-moment ratio Θ is expected to be anomalously low for slow, tsunami earthquakes (Θ ≤ -5.5), but not necessarily anomalous for events that may trigger large-scale slumping. Our energy-duration analysis finds very low values of Θ (Θ ≤ -5.5; Table 1; Fig. 5) for all four known tsunami earthquakes we examine (1992.09.02 Nicaragua, 1994.06.02 Java, 1996.02.21 Peru, 2006.07.17 Java), for a tsunamigenic event (1998.07.17 Papua New Guinea) that is not thought to be a tsunami earthquake (Heinrich *et al.*, 2001; Okal, 2003), for the 2004 Sumatra-Andaman mega-thrust (2004.12.26), and for two interplate (2001.06.23 Peru and 2005.08.16 Honshu) and one intraplate (2001.03.24 Honshu) events.

Rapid application at near teleseismic distances

It is likely that accurate energy-duration results can be obtained more rapidly from observations at closer distances. For the 17 July 2006, M_w=7.7 Java earthquake, the energy-duration procedure applied to 11 *P* to *S* records from stations at 30º to 50º GCD (available within 17 min of OT) produces M_{ED}=7.9 and Θ=-6.0, nearly the same as the values obtained above using about 50 stations at 30º to 90º GCD. In addition, the energy-duration analysis can be terminated before the *S* arrival time for records where the energy integral has converged and the duration measurements are complete. Thus it is likely in practice that the M_{ED} and Θ results will be stable and available within as little as 15 min after OT, a few minutes after the event has been located with teleseismic observations.

Application at regional and local distances

It is also possible that the energy-duration methodology can be applied at local and regional distances when high dynamic-range, high sample-rate data is available. For a preliminary test, we consider 200 sample/sec, strong-motion recordings of the 28 September 2004, M_w=6.0 Parkfield, California earthquake from 5 USGS-GEOS stations in the near-field (distance < 20 km; Borcherdt et al., 2004). Application of our duration estimation as described above, except using f_{cent}=10.0 Hz and a width of 0.5 sec for the envelope smoothing, gives a duration of T_0=8 sec. We apply the energy integral, Eq. (3), with no attenuation factor, with a generalized radiation coefficient $F^{gP}=\langle F^P\rangle$ (since near-field stations see direct *P* energy over much of a moving focal sphere but do not see *pP* or *sP* energy), and including station energy factors $T_0/t_{S\text{-}P}$=7.3 to 3.1 (since at all stations the *S-P* interval, $t_{S\text{-}P}$=1.1 to 2.6 sec, used for energy integration is less than the estimated duration, T_0=8 sec). These modifications, all of which could be preset or determined in real-time, give $M_{ED=}$5.9. Thus the energy-duration values match well the CMT duration of 6 sec and M_w^{CMT}=6.0. **The energy-duration results require data only until just after the *P* arrival time plus the source duration, which for this near-field data set is about 15 sec or less after OT. Thus, in addition to being rapid for routine monitoring, the M_{ED} magnitude determination may be available in close to the early-warning time frame when near-field observations are available.**

6. The 26 December 2004, M9 Sumatra-Andaman mega-thrust earthquake and the 17 July 2006, M7.7 Java tsunami earthquake

For the 2004 Sumatra-Andaman event, bulletins from the PTWC show that the magnitude was evaluated at M_{wp}=8.0 at 15 minutes after OT, and at M_m=8.5 at 1 hour after OT. The final CMT magnitude, available about 3 hours after OT, was M_w^{CMT}=9.0, and, several months after the event, a moment magnitude of M_w=9.1-9.3 was derived from analysis of the Earth's normal modes (*e.g.*, Stein and Okal, 2005; Park, *et al.*, 2005). **The energy-duration magnitude for the 2004 Sumatra-Andaman event is M_{ED}=9.2, a measure which is potentially available within about 20 minutes after OT.** We determine an energy-to-moment ratio parameter Θ=-5.7, a border-line value which would indicate, since this event is an interplate thrust, that it may be a tsunami earthquake. Later study of this event indicates that it was partially a tsunami earthquake (*e.g.*, Seno and Hirata, 2006; Kanamori, 2006), justifying a border-line value for Θ. In any case, given the size and tectonic setting of the event, the high probability that it would generate a major tsunami would be and was recognized rapidly.

For the 2006, Java event, bulletins from the Pacific Tsunami Warning Center (PTWC) show that the event magnitude was evaluated at M_{wp}=7.2 at 17 minutes after OT, and still at *M*=7.2 at about 3 hours after OT. The final CMT magnitude, available about 1 hour after OT, was M_w^{CMT}=7.7, and the CMT message noted that this event had characteristics of a tsunami earthquake. **The energy-duration magnitude for the 2006, Java event, potentially available within 20 minutes after OT, is M_{ED}=7.8. We determine an energy-to-moment ratio parameter Θ=-6.0, a very low value indicating that, since the event is a shallow, interplate thrust, it is has the characteristics of a tsunami earthquake, which is confirmed by later studies (*e.g.* Ammon *et al.*, 2006).**

7. Summary

We have shown that our energy-duration procedure performs well for teleseismic observations at 30° to 90° GCD, producing magnitude estimates M_{ED} that match closely the M_w^{CMT} values for major and great earthquakes (M_w^{CMT} ≥ 7.0), and energy-to-moment ratios Θ that agree with previous results and with the tsunamigenic character of the studied events. The energy-duration methodology may be applicable to smaller events and at regional distances (GCD <~30°), and preliminary application the 2004, Parkfield, California earthquake suggest that the methodology can provide useful information on event size at near-field distances, possibly at close to an early-warning time scale.

Acknowledgements

The work of AL was supported by personal funds. AM and AP were supported in part through the 2005-07 Italian Civil Defense project S4. The IRIS DMC provided access to waveforms used in this study.

References

Ammon, C. J., C. Ji, H.-K. Thio, D. Robinson, S. Ni, H. Kanamori, T. Lay, S. Das, D. Helmberger, V. Hjorleifsdottir, G. Ichinose, J. Polet, D. Wald, 2005. Rupture process of the 2004 Sumatra-Andaman earthquake, *Science*, **308**, 1133-1139.

Ammon, C. J., H. Kanamori, T. Lay, and A. A. Velasco, 2006. The 17 July 2006 Java Tsunami Earthquake (Mw=7.8), (submitted to *Geophys. Res. Lett.*).

Boatwright, J., and G. L. Choy, 1986. Teleseismic estimates of the energy radiated by shallow earthquakes, *J. Geophys. Res.* **91**, 2095–2112.

Borcherdt, R.D., M.J.S. Johnston, C. Dietel, G. Glassmoyer, G. Myren, and C. Stephens, 2004. Acceleration and Volumetric Strain Generated by the Parkfield 2004 Earthquake on the GEOS Strong-Motion Array near Parkfield, CA, *US Geological Survey Open File Report* **2004-1376**, 75pp.

Dziewonski, A.M. and D.L. Anderson, 1981. Preliminary Reference Earth Model (PREM), *Phys. Earth Planet. Inter.* **25**, 297-356.

Dziewonski, A., T.A. Chou, and J. H. Woodhouse (1981. Determination of earthquake source parameters from waveform data for studies of global and regional seismicity, *J. Geophys. Res.*, **86**, 2825-2852.

Haskell, N. A., 1964. Total energy and energy spectral density of elastic wave radiation from propagating faults, *Bull. Seism. Soc. Am.,* **54**, 1811-1841.

Heinrich, P., A. Piatanesi and H. Hebert, 2001. Numerical modelling of tsunami generation and propagation from submarine slumps: the 1998 Papua New Guinea event, *Geophys. J. Int.*, **145**, 97-111.

Hirshorn, B., 2006. *R.H. Hagemeyer Pacific Tsunami Warning Center*, presentation for PTWS-WG1, Intergovernmental Coordination Group for the Pacific Tsunami Warning and Mitigation System (ICG/PTWS), Melbourne, Australia. (http://ioc3.unesco.org/ptws)

Kanamori, H., 2006. The radiated energy of the 2004 Sumatra-Andaman earthquake, *AGU Chapman Vol.*, (in press).

Lomax, A., 2005. Rapid estimation of rupture extent for large earthquakes: application to the 2004, M9 Sumatra-Andaman mega-thrust, *Geophys. Res. Lett.*, **32**, L10314, doi:10.1029/2005GL022437.

Lomax, A. and A. Michelini, 2005. Rapid Determination of Earthquake Size for Hazard Warning, *Eos Trans. AGU*, **86**, 19, 185-189.

Newman, A.V., and E.A. Okal, 1998. Teleseismic Estimates of Radiated Seismic Energy: The E/M_0 Discriminant for Tsunami Earthquakes, *J. Geophys. Res.*, **103** (11), 26,885-98.

Okal, E.A., 2003. T Waves from the 1998 Papua New Guinea Earthquake and its Aftershocks: Timing the Tsunamigenic Slump, *Pure App. Geophys.*, **160**, 1843-1863.

Park, J., *et al.*, 2005. Earth's free oscillations excited by the 26 December 2004 Sumatra-Andaman earthquake, *Science*, **308**, 1139-1144.

Seno, T. and K. Hirata, 2006. Did the 2004 Sumatra-Andaman Earthquake Involve a Component of Tsunami Earthquakes?, *Bull. Seism. Soc. Am.,* **00**, 000-000. (in presss)

Stein, S., and E. A. Okal, 2005. Speed and size of the Sumatra earthquake, *Nature*, **434**, 581-582.

Tsuboi, S., Application of M_{wp} to tsunami earthquake, 2000) , *Geophys. Res. Lett.*, **27**, 3105–3108.

Tsuboi, S., K. Abe, K. Takano, and Y. Yamanaka, 1995. Rapid determination of *Mw* from broadband P waveforms, *Bull. Seism. Soc. Am.*, **85**, 606-613.

Tsuboi, S., P. M. Whitmore, and T. J. Sokolowski, 1999. Application of M_{wp} to deep and teleseismic earthquakes, *Bull. Seism. Soc. Am.*, **89**, 1345-1351.

Vassiliou, M. S., and H. Kanamori, 1982. The energy release in earthquakes, *Bull. Seism. Soc. Am.,* **72**, 371–387.

Weinstein, S., C. McCreery, B. Hirshorn, P. Whitmore, 2005. Comment on "A Strategy to Rapidly Determine the Magnitude of Great Earthquakes" by W. Menke and V. Levin, *Eos Trans. AGU*, **86**, 263, DOI: 10.1029/2005EO280005.